Available online at www.sciencedirect.com
SCIENCE DIRECT®
Optics & Laser Technology 38 (2006) 8–13
Optics & Laser Technology
www.elsevier.com/locate/optlastec

Research on the temperature field in laser hardening

X.F. Wang[a,b,*], X.D. Lu[a], G.N. Chen[b], Sh.G. Hu[a], Y.P. Su[a]

[a] School of Mechanical Engineering and Automation, Beihang University, 37# Xueyuan Road, Haidian District, Beijing 100083, PR China
[b] Chinese Academy of Science, Institute of Mechanics, Beijing 100080, PR China

Received 25 June 2004; received in revised form 9 October 2004; accepted 27 October 2004
Available online 8 January 2005

Abstract

Temperature field in the laser hardening process was numerically simulated by MSC.Marc software. The influence of energy density on laser hardening effect is analyzed. Simulation result is verified through the thermocouple temperature transducer measuring the specimen surface temperature under the laser irradiation. Experimental curves of temperature versus time are in agreement with simulation results. The simulation results can be regarded as a basis for choosing laser technological parameters.

Keywords: Laser hardening; Temperature field; Numerical simulation

1. Introduction

Laser processing is an advanced and highly efficient manufacturing method and has very wide applied perspective in aviation, mechanical engineering and industry of national defense and so on. Laser hardening is a method in which the high-power laser beam quickly irradiates the specimen surface to increase rapidly the specimen surface temperature that is higher than the phase-transformation point and lower than the melting point. After the laser beam is switched off, the cooling base quickly cools the heated region to quench by itself so that the specimen surface is hardened and its performance is modified and improved [1]. Because there is a smaller heat influence region, its heat distortion is small. We can control the surface temperature and hardening depth by adjusting laser beam output power, laser beam moving velocity and the diameter of laser beam spot. Laser hardening can improve the specimen surface rigidity, wearability, toughness and a lot of mechanical performance and ensure the specimen precision. It can realize some special effects that are difficult or not attained with the general heat treatment technique and enhance the specimen lifetime greatly [2].

The facing difficulty is how to choose suitable laser technological parameters in laser surface hardening process so that we can gain the best hardening quality and longest lifetime of the specimen without melting the specimen surface. Hardening effect includes the surface hardness, the depth and the width of the hardening layer. Their value depends on temperature field distribution in the specimen resulting from the specimen surface absorbing laser energy. We measure the surface temperature change by the thermocouple temperature transducer when the laser beam irradiates on the specimen surface. Real-time data are collected by the flexible measure system and the temperature versus time curve is drawn during the hardening process. All results are used to verify the numerical simulation result. The conclusion lays a foundation for realization of the relationship between laser technological parameters and hardening effect and provides training data for using artificial neural network optimizing the laser technological parameters.

*Corresponding author.
E-mail address: wangxiufeng@buaa.edu.cn (X.F. Wang).

0030-3992/$ - see front matter
doi:10.1016/j.optlastec.2004.11.005

2. Experimental method

An experiment has been conducted in the institute of Mechanics, Chinese Academy of Science. The experimental apparatus is the continual output CO_2 laser with 2000 W. The specimen and measuring equipment are shown in Fig. 1a and b. The specimen is chosen as C45 (40 mm × 20 mm × 20 mm) and is put on a workbench. It is continuously irradiated at the center ($y = 10$ mm) and on the edge ($y = 2$ mm) by the laser beam shown in Fig. 2. The laser beam moving velocity is 20 mm/s, the laser beam output power is adjusted to 350 W and the diameter of laser beam spot on the specimen surface is 4 mm. The specimen surface is sprayed with ZirConia in order to enhance absorption of the laser energy. One end of NiCr/NiSi thermocouple is joined to the specimen surface shown in Fig. 2, and the other end is joined to the amplifier adjusting card in order to amplify the voltage signal from mV (from the thermocouple to V shown in Fig. 1c). The data are collected by flexible measure system and the temperature versus time curve is displayed on the computer screen.

After the laser irradiation, the specimen is cut at the irradiated center in a cross section so as to know its micro-organization. We observe the metallographic structure with a NEOPHOT21 metallographic microscope after the sample is rubbed, polished and eroded with 3% nitric acid alcohol. The conclusion provides verified bases for the numerical simulation on laser hardening processes.

3. Numerical simulation

The specimen thickness is cut down to 10 mm in numerical simulation in order to reduce calculation time. Calculated parameters are chosen as experimental parameters. Thermo-physical properties of specimens depend on temperature shown in Fig. 3 [3]. The temperature field in the laser hardening process is numerically simulated with the Galerkin method to solve the instantaneous heat transfer equation in MSC.Marc software.

3.1. Model of calculation

The specimen is discretized by means of an 8-node linear brick element to attain high precision because a steep temperature gradient is produced in the heated region when the laser beam irradiates on the specimen surface. In order to improve efficiency and reduce

Fig. 1. The experimental and measured scheme: (a) the experimental scheme, (b) part amplified view and (c) adjustable amplified board.

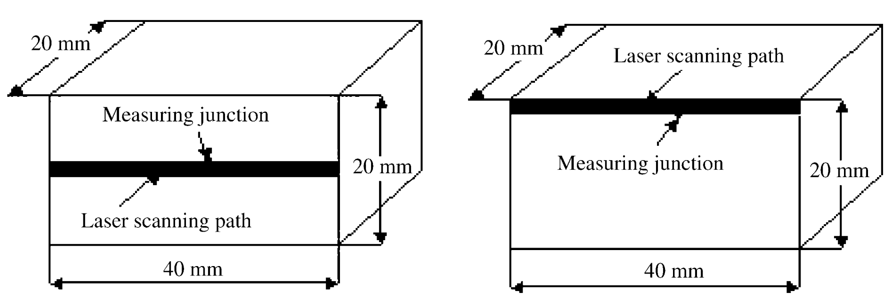

Fig. 2. Specimen size and thermal couple welding position: (a) laser scanning in $y = 10$ mm line and (b) laser scanning in $y = 2$ mm line.

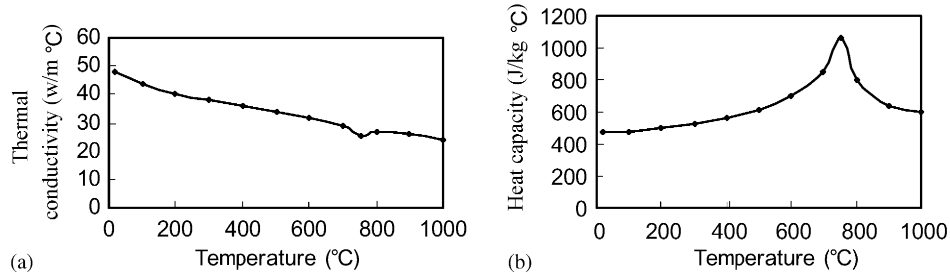

Fig. 3. Thermal properties of C45 versus temperature [3]: (a) thermal conductivity of C45 versus temperature and (b) heat capacity of C45 versus temperature.

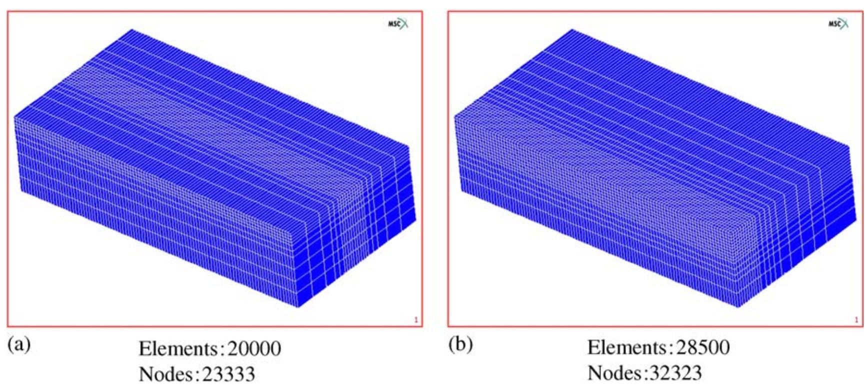

Fig. 4. Divided meshes for FEM calculation: (a) laser scanning in $y = 10$ mm line and (b) laser scanning in $y = 2$ mm line.

calculation, there are dense meshes around the heated region. The size of the mesh is 0.4 mm × 0.4 mm, and there are thin meshes away from the heated region. They are calculated with the following formula:

$$\frac{k\Delta t}{\Delta x^2} \leqslant \frac{1}{2}, \tag{1}$$

where k is the material thermo-diffused efficiency, Δt is the time step, and Δx is the mesh size.

The thickness direction is divided into 10 layers when the laser beam irradiates in the center line ($y = 10$ mm) and 15 layers when the laser beam irradiates in the brink line ($y = 2$ mm), so that there are enough integral points in thickness direction. Meshes in FEM are shown in Fig. 4.

3.2. Boundary condition

Laser beam is input as a stream of heat flux vector and in addition its action position changes with time continuously. Laser beam continuous irradiation is described as jumping and intermittent moving at micro-step intervals [4]. We assume that action position of heat flux only changes with time. The calculated process is simplified. Calculated steps are shown as follows:

It is supposed that the width of sheet metal x is an integral multiple of mesh width Δx. Laser spot moves at Δx distance and remains at t_r time during laser continuous irradiation. Then

$$t_r = \frac{\Delta x}{v}, \tag{2}$$

where v is laser beam moving velocity.

The laser beam goes across a spot distance after $d/\Delta x$ jumps. When the value of Δx is extremely small, we can simulate the laser beam to move continuously.

According to less time of rising temperature and remaining high temperature in laser heating process, we can record information of the temperature field by the short enough step of time. So heat flux density distribution in the circular spot is regarded to be uniformity within each t_r. The heat flux density is

$$q = \frac{4AP}{\pi d^2}, \tag{3}$$

where A is the absorption coefficient of sheet metal ($A = 0.55$), and P is the laser beam output power.

Laser beam jumping and intermittent moving at micro-step intervals on the specimen surface is simulated by FLUX subroutine in MSC.Marc software. Automatic loading is realized and the calculated effect is improved.

The specimen cools in air after laser irradiation. β is regarded as total heat exchange coefficient including convection and irradiation. The lost energy for heat exchange can be calculated with the following formula:

$$q_h = \beta(T - T_0), \quad (4)$$

where T_0 is the room temperature in lab ($T_0 = 25\,^\circ\mathrm{C}$).

Value of β changes with temperature in steady condition [5]. In order to cause deep temperature gradient in the heated region after laser beam irradiated on the specimen surface, value of β is adjusted 80–100 times of the value in steady condition [6]. But we think that it is difficult to determine the value of β, it not only increases with surface temperature gradient's increase but also depends on section size of the specimen and cooling time. Value of β is corrected by our experimental results [2] shown in Table 1.

Table 1
Total heat exchange coefficient

Temperature (°C)	β[5]$(\mathrm{W(m^2\,K)^{-1}})$	β[6]$(\mathrm{W(m^2\,K)^{-1}})$	β[2]$(\mathrm{W(m^2\,K)^{-1}})$
20	6	480–600	90,000
300	50	4000–5000	59,000
600	120	9600–12,000	51,000
750	180	14,400–18,000	49,000
900	200	16,000–20,000	47,500
1200	250	20,000–25,000	42,000
1500	370	30,240–37,800	32,500

The subroutine of total heat exchange boundary condition is programmed by FORTRON language. Value of β versus temperature is the input by FILM user subroutine.

4. Results and discussion

Temperature versus time on the surface measured junction is shown in Fig. 5. The depth and width of the hardening layer are compared in Fig. 6.

Fig. 5 indicates that the change trend and the maximum point in the calculated curve are approximate to the experimental curve. The hardening effect is changed when the laser beam irradiates on the specimen brim because heat insulation boundary holds back heat transfer and the brim; temperature increases resulted from reflection and overlying. We must select appropriate laser parameters to control the specimen brim temperature so as to prevent the specimen surface changing from brim overheating and specimen lifetime decreasing from unhardened brim. The form and size of the hardening layer in simulation results are in accordance with the experimental result shown in Fig. 6.

It can be proved that the calculated model and parameters are reasonable. We can analyze by simulation how the change of energy density influences the laser hardening effect.

During laser beam irradiation, the surface heating temperature must be between the phase-transformation point and the melting point in order to attain good

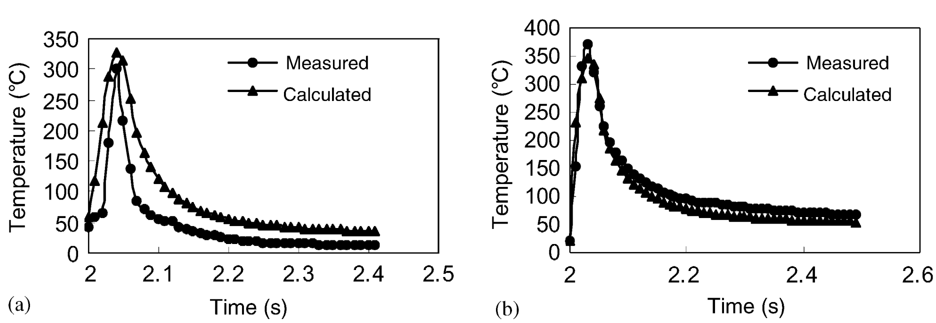

Fig. 5. Measuring junction temperature versus time: (a) laser scanning in $y = 10$ mm line and (b) laser scanning in $y = 2$ mm line.

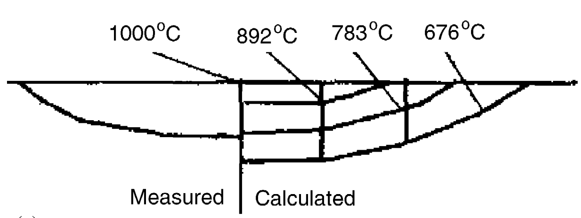

(a)

Hardened size	Calculated	Measured
Depth (mm)	0.2	0.2
Width (mm)	1.8	1.7

(b)

Fig. 6. Laser scanning in $y = 10$ mm line of the simulation result compared with experimental result: (a) temperature field and (b) hardened depth and width.

performance on quenching surface. The phase-transformation point is regarded as 794 °C because it will rise versus heating velocity. Generally the surface temperature is lower than 1200 °C. We should keep the surface temperature between 794 °C and 1200 °C depending on the energy density selected. The isotherm depends on the calculation result. The width and depth of the hardening layer can be estimated by the isotherm. The results are shown in Table 2.

Table 2 indicates that the maximum temperature on the specimen surface increases with the laser beam output power improvement and the depth and width of the hardened layer increases with it, too.

The form and size of the hardened layer will change with the laser beam output power, the laser beam moving velocity and the laser beam spot diameter changes although the laser energy density is constant. The experimental parameters are shown in Table 3.

Table 3 indicates that:

(1) When the laser beam output power is constant, the laser beam moving velocity is slower and the laser beam spot diameter is larger, the highest surface temperature obviously drops and the depth and width of the hardened layer obviously reduce. The slower moving velocity means irradiation time is longer on the specimen surface and more energy is absorbed by the specimen surface. The larger laser beam spot diameter means less power density is absorbed by the specimen surface. The synthetic effect shows that the laser beam spot diameter has more effect than the laser beam moving velocity.
(2) When the laser beam moving velocity is constant, the laser beam output power is lower and the laser beam spot diameter is smaller, the highest surface temperature obviously increases and the depth and width of the hardened layer obviously reduce due to smaller heated region. The smaller laser beam spot diameter means more power density is absorbed by the specimen surface. The lower laser beam output power means less energy is absorbed by the specimen surface. The synthetic effect shows that the laser beam spot diameter has more effect than the laser beam output power.
(3) When the laser beam spot diameter is constant, the laser beam output power is lower and the moving velocity is slower, the highest surface temperature obviously drops and the depth and width of the hardened layer obviously reduce. The slower moving velocity means that the irradiation time is longer on the specimen surface and more energy is absorbed by the specimen surface. The lower laser beam output power means less power density is absorbed by the specimen surface. The synthetic effect shows that the laser beam output power has more effect than the laser beam moving velocity.

Table 2
The highest surface temperature, hardened depth and width of the specimen

Energy density (J/mm^2)	5.14	4.38	3.57
Highest surface temperature (°C)	1242	997	808
Depth (mm)	0.3	0.2	<0.1
Width (mm)	2.66	1.8	<0.8

Table 3
The highest surface temperature, hardened depth and width of the specimen

Power (W)	175	350	260	260	440
Scanning speed (mm/s)	20	20	15	30	25
Diameter (mm)	2	4	4	2	4
Highest surface temperature (°C)	1540	997	915.5	2108	1271
Depth (mm)	0.33	0.2	0.1	—	0.33
Width (mm)	1.6	1.8	1.6	—	2.8

5. Conclusion

The numerical simulation repeats the processes of the laser hardening. The simulation precision is improved because the recorded real-time temperature on the specimen surface is compared with the simulation result. The form and size of the hardened layer is predicted by numerical simulation. The power density influence on the laser hardening effect is analyzed quantitatively.

With the increase in laser power density, the highest temperature on the specimen surface is higher so that the depth and width of the hardened layer increases. When the laser beam energy density is constant, the form and size of the hardened layer will change combined with different parameters of the laser beam output power, the laser beam moving velocity and the laser beam spot diameter. The sequence of laser technological parameters influencing the hardening effect is shown as follows: the laser beam spot diameter → the laser beam output power → the laser beam moving velocity. We can choose suitable laser technological parameters for the hardening effect in engineering based on the working condition of workpieces. The numerical simulation results can provide basic parameters in engineering and training data for using artificial neural network optimizing the laser technological parameters. Those research results will be discussed in other papers.

Acknowledgements

The authors would like to acknowledge the China National Science Foundation and China Aviation

National Science Foundation for supporting their research.

References

[1] William MS. Laser material processing, 2nd ed. New York: Springer; 1998.
[2] Wang Xiufeng. Application of laser non-melting processing technology in the sheet metal forming. PhD Dissertation, Beijing University of Aeronautics and Astronautics, 2003.
[3] Tan Zhen, Guo Guangwen, editors. Thermo-physical properties of engineering alloy. Published by Metallurgical industry Publisher; 1994. 9pp.
[4] Ji Zhong. Laser sheet metal forming and simulation. PhD Dissertation, Xi'an, Northwestern Polytechnical University, 1997.
[5] Liu Shunhong, et al. Study on numerical of the temperature field in laser welding of steel sheet. Weld mach 2001;8:16–9.
[6] Jiang Eenqiu. Transient shock effect of heat transfer, mass diffuse and momentum transfer. Mascow:Science Publisher; 1997. 2pp.